

COVALENT FUNCTIONALIZATION OF SINGLE WALLED CARBON NANOTUBES WITH DOXORUBICIN FOR CONTROLLED DRUG DELIVERY SYSTEMS

C. C. CIOBOTARU^{a*}, C. M. DAMIAN^b, S. POLOSAN^a, E. MATEI^a, H. IOVU^b

^aNational institute of Materials Physics, Atomistilor 105 bis, 077125, Magurele, Bucharest, Romania

^bUniversity POLITEHNICA of Bucharest, Faculty of Applied Chemistry and Materials Science, Calea Victoriei 149, 010072, Bucharest, Romania

The objective of this study was to obtain nanocomposites based on SWCNTs functionalized with carboxyl groups and doxorubicin (DOX) as a chemotherapeutic drug through covalent bonds formed by carboxyl groups from SWCNTs and amino groups from DOX. The formation of these nanocomposites was proved by using different characterization methods like Fourier transform Infrared spectroscopy and X-ray photoelectron spectroscopy (XPS). Also thermogravimetric analysis was employed to study the thermal behavior of our nanocomposites. X-ray diffraction and Raman spectroscopy revealed that the surface was modified by the covalent bonding of DOX to SWCNTs. The in vitro drug release was studied by using UV-VIS Spectroscopy.

(Received January 31, 2014; Accepted March 24, 2014)

Keywords: SWCNTs, DOX, covalent functionalization, UV-VIS, XPS,

1. Introduction

Since they were discovered carbon nanotubes (CNTs) have been considered an ideal material for a large range of applications due to their unique properties [1]. Carbon nanotubes represents a graphitic nanomaterial having high dimensional ratio, lengths from nanometers to micrometers and diameters of 0.4 to 2 nm for single-walled carbon nanotubes (SWCNTs) and 2-100 nm for multi-walled carbon nanotubes (MWCNTs). These structures have wide range of properties such as mechanical, electronic, thermal, optical and pharmaceutical [2-6] but the most important one is the biomedical application of these materials [7-8].

The using of CNTs in biomedical and biological applications requires a better solubility in aqueous media. This was a major technical barrier that has been broken after the discovery of functionalization methods of CNTs [9-10].

SWCNTs are widely used in drug delivery systems due to its sp^2 hybridization surface and its large surface area that can be loaded with a high amount of drugs. Also its internal diameter makes SWCNTs a good carrier for drugs that can be encapsulated inside the walls [11-12].

The chemotherapy is one of the methods in cancer treatment that involves the destruction of cancer cells with minimal side effects to healthy tissues [13].

The anthracycline, doxorubin (DOX), is one of the drugs that are widely used in chemotherapy due to its efficacy in fighting a wide range of cancers, particularly in treatment of breast cancer [14-15].

Zhuang Liu [16] et al. described a method of activation of SWCNTs with DOX. First they PEGylated SWCNTs and after the pegylation they loaded DOX onto SWCNTs by supramolecular π - π stacking.

The aim of this study is the functionalization of the carboxyl groups from SWCNTs surface by covalent bonding with amino groups from DOX, using an activation system based on 1-(3-Dimethylaminopropyl)-3-ethylcarbodiimide (EDC) and N-Hydroxysuccinimide (NHS) and to

* Corresponding author: claudiu.ciobotaru@infim.ro

release this drug in phosphate buffer solution. These new obtained nanocomposite materials were characterized using different techniques like spectroscopic methods (XPS, FTIR, RAMAN and UV-VIS), thermogravimetric analysis (TGA), X-Ray diffraction (XRD) and scanning electron microscopy (SEM).

2. Materials and methods

2.1 Materials

SWCNTs purified for 48 h and functionalized with carboxyl groups by oxidation were obtained as previously described [17] named as SWCNTs-p48h-Ox and were used in the activation process with 1-(3-Dimethylaminopropyl)-3-ethylcarbodiimide (EDC), and N-Hydroxysuccinimide (NHS) purchased from Sigma-Aldrich.

Doxorubicin (DOX) the antitumor drug was received from Sigma Aldrich and was used without any purification or modification.

PBS (phosphate buffer solution) having pH=5.5 was obtained from 2 solutions. First solution contains 13.61 g potassium dihydrogen phosphate diluted in 1000 ml flask containing distilled water. Second solution contains 35.81 g disodium hydrogen phosphate diluted in 1000 ml flask containing distilled water. To obtain PBS with pH=5.5, 96.4 ml of solution I and 3.6 ml of solution II were mixed.

Dialysis sacks obtained from cellulose having inflated diameter approx. 21 mm and pore size 12000 Da MWCO were purchased from Sigma Aldrich.

2.2 Methods

2.2.1 Activation with Doxorubicin of SWCNTs-48h-Ox

The activation of SWCNTs-p48h-Ox with DOX was done using EDC and NHS. Briefly 7.5 mg of EDC were dissolved in 5 ml of PBS having pH 5.5. After dissolving 15 mg of SWCNTs p48hOx were added. Then 22.5 mg of NHS were added and the mixture was sonicated 30 min at room temperature. After 30 min, 7.5 mg of DOX were added and the sonication continued for another 90 min at room temperature in the dark. When the sonication was finished the solution was filtered and the resulted solution was analyzed at UV-VIS to determine the amount of DOX that was covalently bonded to the SWCNTs surface. The resulted nanocomposites were dried at vacuum oven for 48h. From the calibration curve and the absorbance of the washing solution it results that on the SWCNTs surface approximately 5.72 mg of DOX was covalently bonded (figure 1).

$$DOX - loading\ efficiency\ (\%) = 100 \frac{(W_{feed}DOX - W_{free}DOX)}{W_{feed}DOX} = 76\%$$

2.2.2 The release of Doxorubicin covalently bonded onto the SWCNTs surface.

After activation the amount of SWCNT with DOX obtained was dispersed in 5 ml of PBS pH=5.5 and it was sonicated for 2 min for a better dispersion. Then the solution was introduced into a dialysis sack. The dialysis sack was previously washed with PBS 5.5 to remove all the impurities.

The dialysis sack containing the solution of SWCNTs with DOX and PBS was closed to both ends and immersed in a glass which contains 50 ml of PBS 5.5. The glass was introduced in a thermostated shaking bath for liquids at 37 °C and the rotation speed was set to 75 rpm.

From time to time 3 ml of solution were extracted and analyzed at UV-VIS equipment. This volume was replaced with another 3 ml of fresh PBS 5.5.

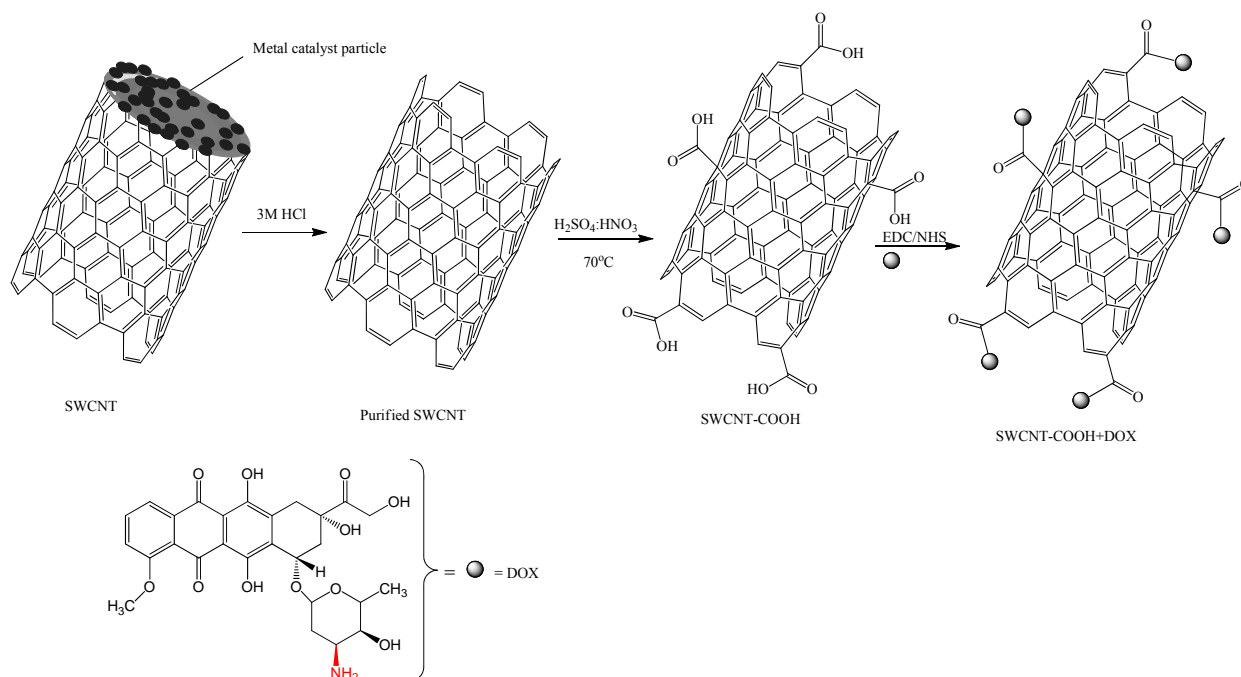


Fig. 1. Reaction of purification, oxidation and activation process of SWCNTs with DOX

2.3 Advanced characterization

Fourier transform infrared spectroscopy (FTIR) spectra of SWCNTs, purified SWCNTs, oxidized SWCNTs and activated SWCNTs with DOX were registered on a Bruker Vertex 70 equipment in 400 ÷ 4000 cm⁻¹ range with 4 cm⁻¹ resolution and 32 scans. The samples were analyzed in KBr pellets.

Raman spectra of the samples were recorded on a DXR Raman Microscope (Thermo Scientific) by 532 nm laser line. The 10x objective was used to focus the Raman microscope.

Thermogravimetry analysis (TGA) of the samples was done on Q500 TA equipment, using nitrogen atmosphere from 20 °C to 600 °C with 10 °C/min heating rate.

The X-ray photoelectron spectroscopy (XPS) spectra were recorded on Thermo Scientific K-Alpha equipment, fully integrated, with an aluminum anode monochromatic source. Survey scans (0-1350 eV) were performed to identify constitutive elements.

The X-Ray diffraction measurements have been performed on a BRUKER D8 ADVANCE type X-ray diffractometer, in focusing geometry, with a vertical theta-theta goniometer and horizontal sample carrier. The instrument is equipped with copper target X-ray tube with CuK_{α1} radiation ($\lambda_{\text{CuK}\alpha 1} = 1.5406 \text{ \AA}$) and nickel K β filter. Lynx-Eye one-dimensional detector ensures a collection rate with two orders of magnitudes higher than that of conventional point detectors and very good angular resolutions. The working parameters are 40 kV and 40 mA. The 2 θ scan range was set to 5–50° with a step size of 0.04° and a resolution of 0.01°.

UV-Vis absorbance of DOX was measured at $\lambda = 480 \text{ nm}$ on a UV-3600 Shimadzu equipment provided with a quartz cell having a light path of 10 mm and equipped with a Syringe Sipper Type N.

Scanning electron micrographs were obtained using a Zeiss EVO 50 SEM having LaB6 cathode with Bruker EDX system.

3. Results and discussion

3.1 XPS Analysis

The XPS analysis was employed to analyze the chemical composition at the surface of SWCNTs, purified SWCNTs, oxidized SWCNTs and covalent activated SWCNTs with DOX.

From XPS spectrum of SWCNTs purified at 48h it can be observed that the intensity peak of Mo3d decreases after purification process. Also the spectrum for SWCNTs purified and oxidized showed that the intensity peak of O1s increases after oxidation [17].

For SWCNTs purified, oxidized and activated with DOX spectrum it can be noticed the increase in intensity for N1s peak from amino groups presented in DOX structure.

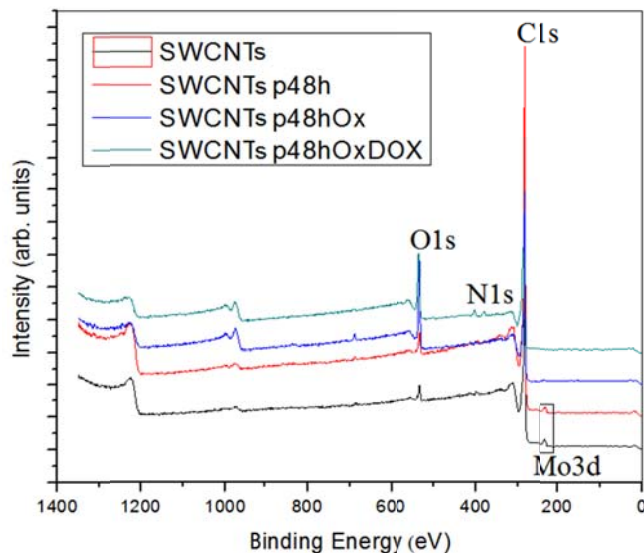


Fig. 2. XPS spectra of SWCNTs, SWCNTs-p48h, SWCNTs-p48h-Ox, SWCNTs-p48h-Ox+DOX

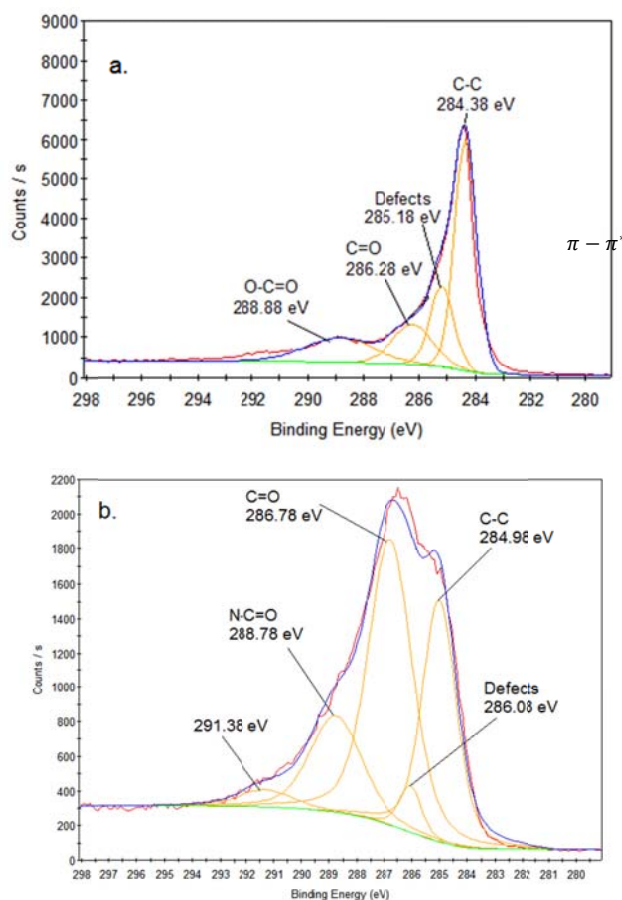


Fig. 3. Deconvolution of C1s for a. SWCNTs-p48h-Ox and b. SWCNTs-p48h-Ox covalently functionalized with DOX

The deconvolution of C1s for SWCNTs-p48h-Ox+DOX presents different shape due to the surface modification by transforming O-C=O bonds represents by peak from 288.88 eV, as binding energy shift from C-C bonds (4.5 eV) (figure 3. a.) into N-C=O bonds from 288.78 eV, as binding energy shift from C-C bonds (4 eV) (figure 3. b.). This modification is responsible to the covalent activation of SWCNTs-p48h-Ox with DOX by forming C-N bonds between C from COOH and N from NH₂ groups.

In table 1 the atomic percentages of elements that were detected in analyzed samples are shown. It can be observed the decrease of C 1s atomic percent due to the increase of O 1s after oxidation process. Also the presence of F 1s in XPS spectra of SWCNTs can be explained by the use of PTFE membranes for filtration process.

Table 1. XPS data for SWCNTs, SWCNTs-p48h, SWCNTs-p48h-Ox, SWCNTs-p48h-Ox+DOX

Samples	SWCNTs	SWCNTs-p48h	SWCNTs-p48h-Ox	SWCNTs-p48h-Ox+DOX
At %				
C1s	96.43	96.09	79.91	71.07
O1s	3.25	3.78	18.97	25.91
Mo3d	0.32	0.13	0	0
F1s	0	0	1.12	0.91
N1s	0	0	0	2.13

3.2 FT-IR Spectroscopy

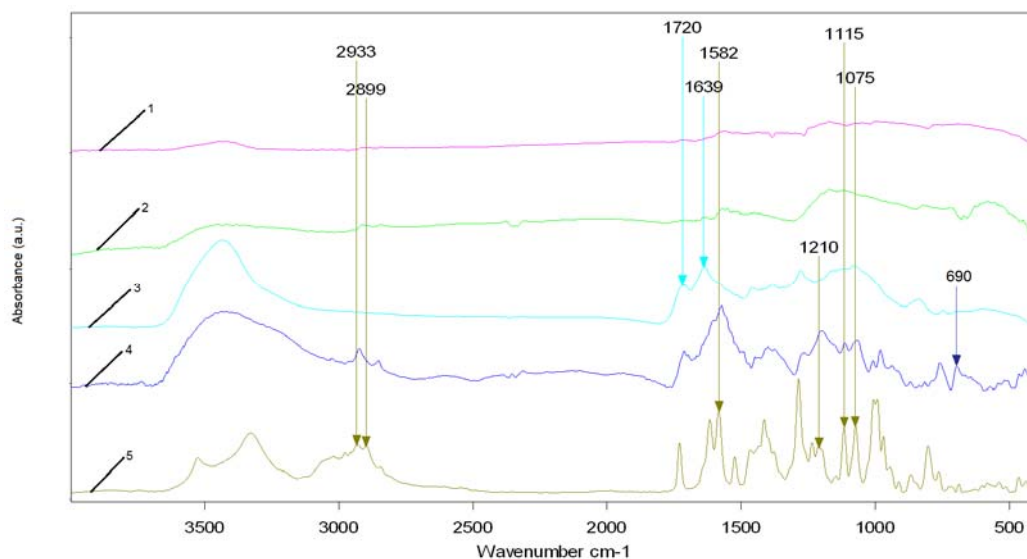


Fig. 4. FT-IR spectra for 1) SWCNTs, 2) SWCNTs-p48h, 3) SWCNTs-p48h-Ox, 4) SWCNTs-p48h-Ox+DOX and 5) Doxorubicin

From FT-IR spectrum representing the SWCNTs-p48h-Ox (curve 3 from Figure 4) it can be observed the appearance of two new peaks at 1720 cm⁻¹ and 1639 cm⁻¹ corresponding to C=O stretching vibration bonds. Spectrum 4 representing the SWCNTs-p48h-Ox+DOX shows the appearance of new peaks responsible to DOX structure that was covalently bonded on SWCNTs. The peak from 690 cm⁻¹ represents the deformation vibration of NH bonds and peak from 1210 cm⁻¹ is corresponding to C-N bonds which are newly formed by the reaction with DOX. The spectrum 5 representing DOX presents many peaks that can be seen also in spectrum 4 meaning that the DOX structure was not affected during the activation process. Also the appearance of these peaks proves the DOX loading on SWCNTs [18].

3.3 Raman Spectroscopy

The Raman spectroscopy gives us the information about the modifications of the structure and the differences between I_D/I_G ratios of the samples.

It was observed that I_D/I_G ratio exhibits a small value for as-received SWCNTs but it increases slightly after purification reaction due to the removing of metal particles of catalyst and amorphous carbon.

After oxidation reaction (spectrum 3) the I_D/I_G ratio increases up to 0.8 meaning that the SWCNTs surface was modified by the introducing of COOH groups.

The SWCNTs-p48hOx+DOX shows a small increase close to 0.9 due to the binding of DOX to COOH groups from SWCNTs by forming C-N bonds [19].

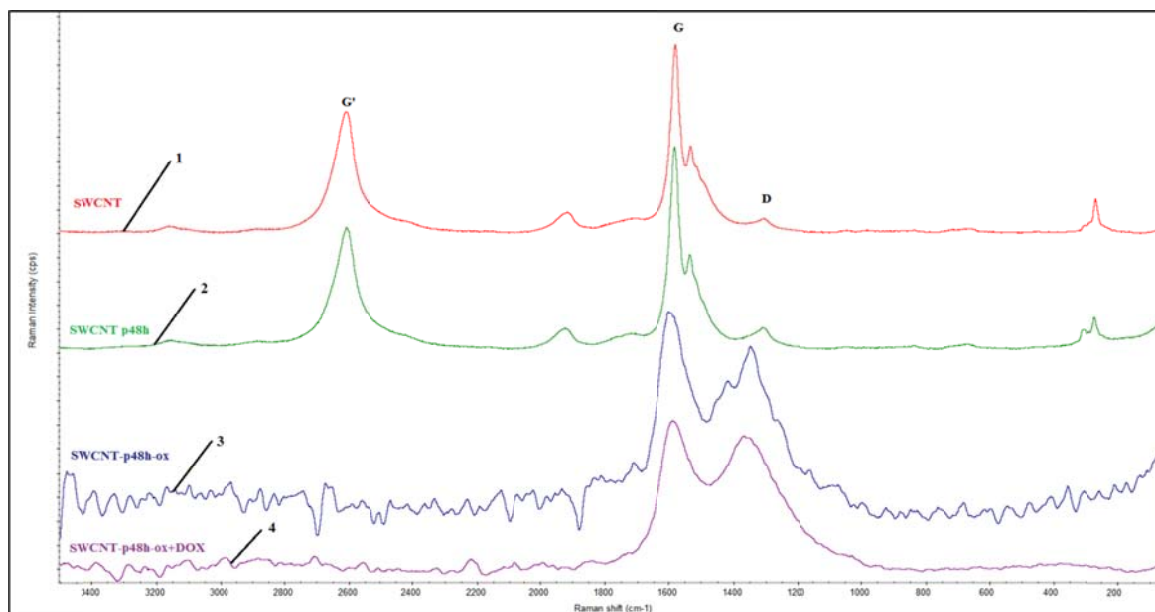


Fig. 5. Raman spectra for 1) SWCNTs, 2) SWCNTs-p48h, 3) SWCNTs-p48h-Ox, 4) SWCNTs-p48h-Ox+DOX

Table 2. I_D/I_G ratio for SWCNTs as-received, purified, oxidized and activated with DOX

Sample	I_D	X_D	I_G	X_G	I_D/I_G
SWCNTs	115.01	1308.27	1556.38	1581.15	0.074
SWCNTs-p48h	174.21	1311.02	1679.12	1582.94	0.104
SWCNTs-p48h-Ox	226.88	1349.59	284.72	1598.37	0.797
SWCNTs-p48h-Ox+Dox	128.04	1370.19	142.86	1588.11	0.896

3.4 Thermogravimetric analysis

The thermogravimetric analysis was performed to observe the thermal behavior and to calculate the mass loss. It was observed that as-received SWCNTs loss 6.2% of mass at 600°C. This demonstrates that SWCNTs have a good thermal stability. The SWCNTs purified have a smaller thermal stability losing 11.8% of mass but have the same thermal behavior like SWCNTs as-received. This small mass loss proves that the amorphous carbon and metals particle from catalyst were removed but also that the structure of SWCNTs was not affected during the purification process.

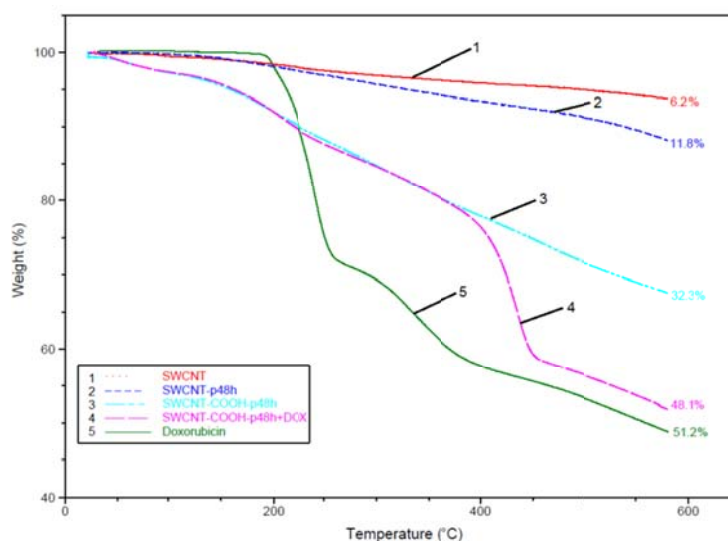


Fig. 6. TG curves for 1) SWCNTs, 2) SWCNTs-p48h, 3) SWCNTs-p48h-Ox, 4) SWCNTs-p48h-Ox+DOX and 5) Doxorubicin.

The SWCNTs-p48hOx (curve 3) shows different thermal behavior due to the decarboxylation and dehydrogenation of $-\text{COOH}$ groups from SWCNTs surface near to 200°C and the mass loss is approximately 32%. After covalent activation the curve 4 representing SWCNTs-p48hOx and covalently activated with DOX exhibits 3 steps: the first stage is attributed to the amino bonds dissociation and the decarboxylation and dehydrogenation of $-\text{COOH}$ groups near to 200°C . The second stage is assigned to the degradation of DOX between $350 - 500^{\circ}\text{C}$ and the third stage corresponds to the degradation of SWCNTs. The mass loss of this sample was 48% due to the degradation of carboxyl groups and DOX [20].

3.5 X-Ray Diffraction

The XRD data for SWCNTs, SWCNTs-p48h, SWCNTs-p48h-Ox, SWCNTs-p48h-Ox+DOX are presented in table 3. The dimension of the nanotubes were calculated using the formula: $D = \frac{K * \lambda}{\beta * \cos(\theta)}$, where D are the dimension of the nanotubes on (002) direction, $\lambda = 1.54 * 10^{-10}$ m and β is half-width in radian. K is constant = 0.9.

Table 3. XRD data for SWCNTs as-received, purified, oxidized and activated with DOX.

Sample	2θ ($^{\circ}$)	$2\theta/2$ ($^{\circ}$)	$\text{Cos}(2\theta/2)$	Half-width in grade	Half-width in radian	Half-width $*\text{cos}(2\theta/2)$	D	D*100 in nm
SWCNTs	25.71	12.85	0.97	2.20	38.37	37.226	0.0372	3.72
SWCNTs-p48h	25.74	12.87	0.97	2.33	40.64	39.426	0.0351	3.51
SWCNTs-p48h-Ox	25.7	12.85	0.97	2.35	40.99	39.764	0.0348	3.48
SWCNTs-p48h-Ox+DOX	25.74	12.87	0.97	1.96	34.19	33.165	0.0417	4.17

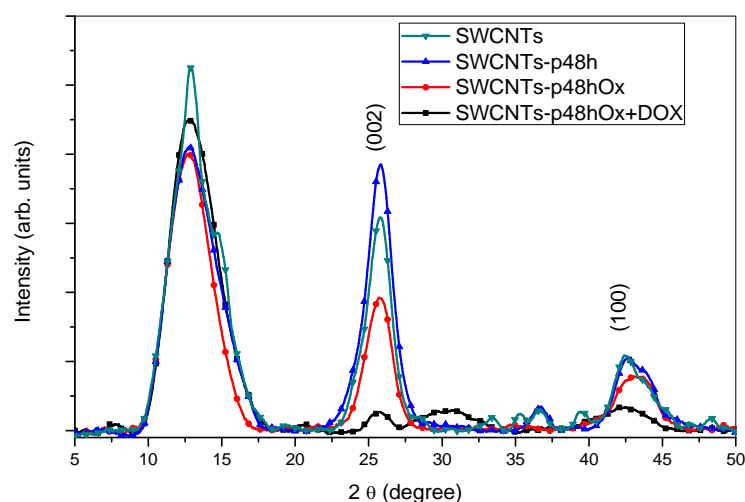


Fig. 7. XRD patterns for SWCNTs, SWCNTs-p48h, SWCNTs-p48h-Ox and SWCNTs-p48h-Ox+DOX

It was observed that the dimension decreases after purification due to the removal of amorphous carbon and Mo3d. This decrease is also presented in SWCNTs-p48hOx dimension due to the extreme oxidation condition which removes all the Mo3d quantity. From SWCNTs-p48hOx+DOX it was observed an increase of the dimension meaning that the surface of the nanotubes was successfully covalently functionalized with DOX [21]. These results are related to Raman data.

3.6 Ultraviolet visible spectroscopy (UV-VIS)

Comparing with Cisplatin the DOX is one of the drugs that gives signal in UV-VIS. Using the UV-VIS absorbance from 480 nm it was calculated the amount of drug that was released at different times [22]. The drug release profile is presented in figure 8. It can be noticed that the drug started to release slowly, after 7 days 7.3% being released. The release stopped after 36 weeks when the amount of DOX released was 31 %.

This slow release of DOX from SWCNTs can be explained by the impossibility of breaking C-N bonds formed during the activation reaction. However, this long time release proves that some of the C-N bonds were broken.

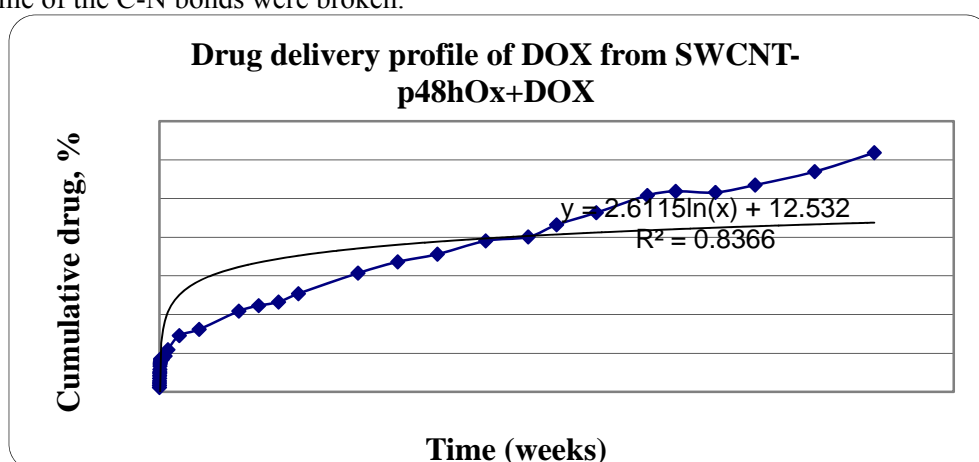


Fig. 8. Delivery profile of DOX from SWCNTs-p48hOx+DOX

3.7 Scanning electron microscopy (SEM)

In order to evaluate the surface modification of SWCNTs after oxidation and activation with DOX the obtained nanocomposites were examined by SEM (figure 9).

Figure 9 (a) shows short nanotubes with open end caps due to the higher density of functional groups in this area, confirming that the oxidation was successfully realized. In this way

the SWCNTs-p48h-Ox are just prepared for the future covalent functionalization with DOX molecules.

The SEM image from figure 9 (b) shows big blocks. The carbon nanotubes cannot be observed due to the polymeric activation system components formed by EDC and NHS that cover the obtained systems. It is suggested that the SWCNTs-p48h-Ox is embedded in the polymeric activators. Also the white spots can be assigned to doxorubicin molecules that were covalently bonded on SWCNTs surface.

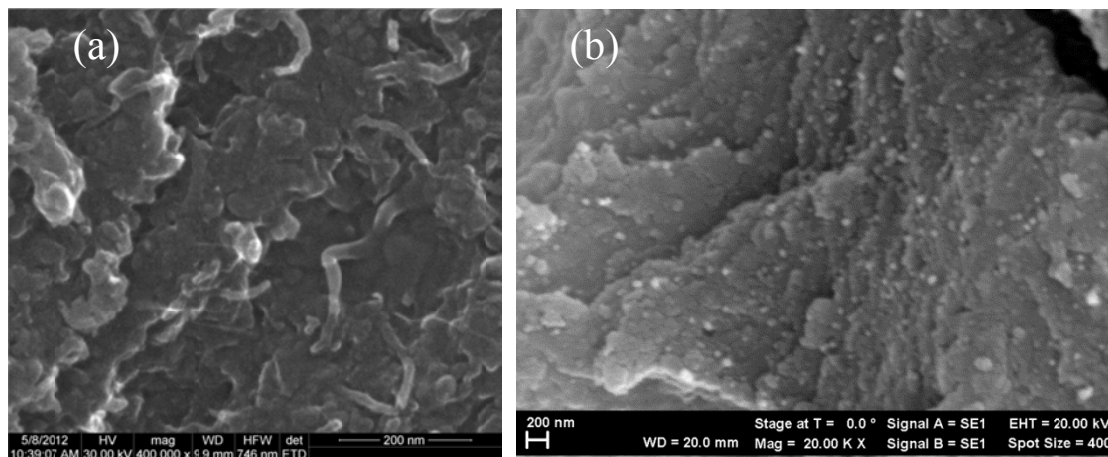


Fig. 9. SEM images of SWCNTs-p48hOx (a) and SWCNTs-p48hOx+DOX (b)

4. Conclusions

The SWCNTs previously purified for 48 h and oxidized were successfully functionalized with doxorubicin by covalent bonding. The process of forming of covalent bonds between the activated oxidized SWCNTs and DOX molecules was proved by FT-IR, Raman and XPS.

The release of DOX from SWCNTs-DOX systems is a very slow process considering the very tough C-N bonds formed during the reaction between SWCNTs and DOX.

SEM method was not useful in this case to show a detailed morphology of SWCNTs-DOX systems formed because of the activators molecules of EDC and NHS used for activation the oxidized SWCNTs which cover almost entirely the SWCNTs

Acknowledgement

The work has been funded by the Sectoral Operational Programme Human Resources Development 2007-2013 of the Romanian Ministry of Labour, Family and Social Protection through the Financial Agreement POSDRU/107/1.5/S/76903.

References

- [1] S. Ijima, Nature, 354, (1991).
- [2] J. N. Coleman, U. Khan, W. J. Blau, Y. K. Gun'ko, Carbon, **44**(9), (2006).
- [3] P.L. Lai, S.C. Chen, M.F. Lin, Physica E: Low-dimensional Systems and Nanostructures, **40**(6), (2008).
- [4] Z. Han, A. Fina, Progress in Polymer Science, **36**(7), (2011).
- [5] R.B. Chen, C.H. Lee, C.P. Chang, C.S. Lue, M.F. Lin, Physica E: Low-dimensional Systems and Nanostructures, **34**(1-2), (2006).
- [6] M. Foldvari, M. Bagonluri, Nanomedicine: Nanotechnology, Biology, and Medicine, **4**(3), (2008).
- [7] S. Peretz, O. Regev, Current Opinion in Colloid & Interface Science, 17 (2012).
- [8] B. S. Wong, S. L. Yoong, A. Jagusiak, T. Panczyk, H. K. Ho, W. H. Ang, G. Pastorin, Advanced Drug Delivery Reviews, **65**(15), 2013

- [9] C. Zhang, W. Zhu, L. Gao, Y. Chen, *Chinese Journal of Polymer Science*, **29**(6), (2011).
- [10] Z. Liu, K. Chen, C. Davis, S. Sherlock, Q. Cao, X. Chen, H. Dai, *Cancer Res*, **15**(68), (2008).
- [11] L. Meng, X. Zhang, Q. Lu, Z. Fei, P. J. Dyson, *Biomaterials* **33**(6), (2012).
- [12] U. Arsawang, O. Saengsawang, T. Rungrotmongkol, P. Sornmee, K. Wittayanarakul, T. Remsungnen, S. Hannongbua, *Journal of Molecular Graphics and Modelling* **29**(5), (2011).
- [13] A. Guven, I. A. Rusakova, M. T. Lewis, L. J. Wilson, *Biomaterials* **33**(5), (2012).
- [14] L. Y. Lin, N. S. Lee, J. Zhu, A. M. Nyström, D. J. Pochan, R. B. Dorshow, K. L. Wooley, *Journal of Controlled Release*, **152**(1), (2011).
- [15] T. Murakami, J. Fan, M. Yudasaka, S. Iijima, K. Shiba, *Molecular Pharmaceutics*, **3**(4), (2006).
- [16] Z. Liu, A. C. Fan, K. Rakhra, S. Sherlock, A. Goodwin, X. Chen, Q. Yang, D. W. Felsher, H. Dai, *Angew Chem Int Ed Engl*. **48**(41), (2009).
- [17] C. C. Ciobotaru, C. M. Damian, H. Iovu, *U.P.B. Sci. Bull., Series B*, **75**(2), (2013).
- [18] D. Depan, J. Shah, R.D.K. Misra, *Materials Science and Engineering C*, **31**(7), (2011).
- [19] M. M. Stylianakis, J. A. Mikroyannidis, E. Kymakis, *Solar Energy Materials & Solar Cells*, **94**(2), (2010).
- [20] Q. Zhang, W. Li, T. Kong, R. Su, N. Li, Q Song, M. Tang, L. Liu, G. Cheng, *Carbon*, **51**, (2013)
- [21] D. Ma, J. Lin, Y. Chen, W. Xue, L. Zhang, *Carbon*, **50**, (2012).
- [22] Z. Liu, X. Sun, N. Nakayama-Ratchford, H. Dai, *ACSNANO*, **1**(1), (2007).